Supplementary figure 1
Preservation of flow karyograms following FISH.

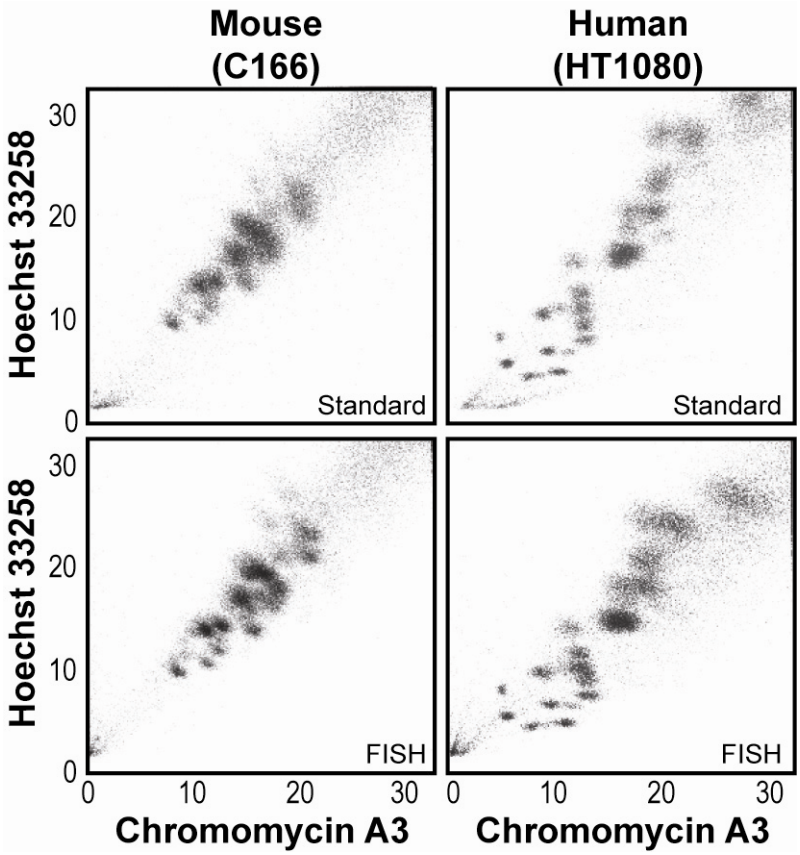

Hoechst 33258/Chromomycin A3 bivariate flow karyotypes of chromosomes isolated from cell lines originating from mouse (C166) and human (HT1080) using the polyamine method before (Standard) and after denaturation in 70% formamide at 80°C for 5 minutes (FISH).

Supplementary figure 2
Hybridization specificity of PNA probes by chromosome flow FISH.

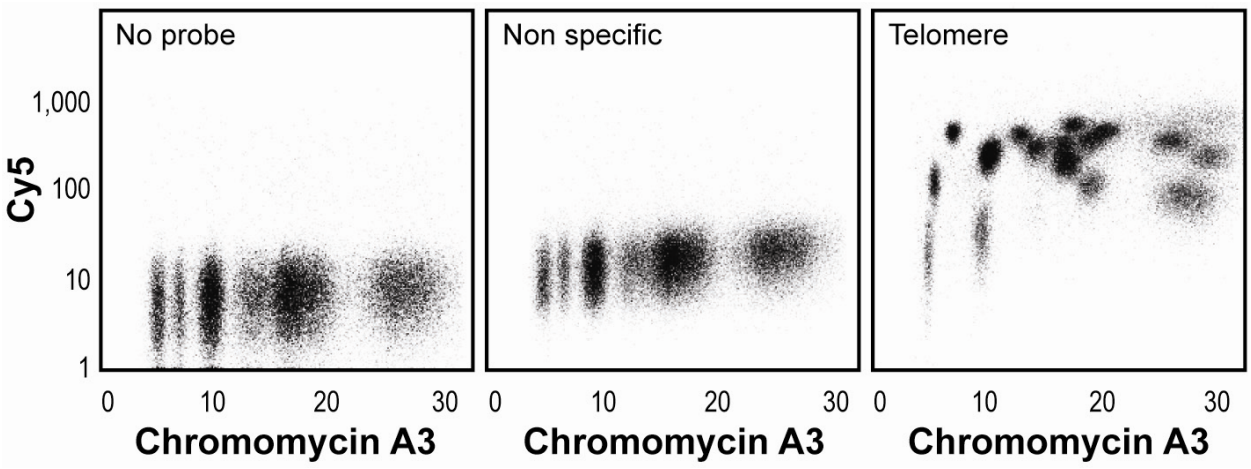

Chromosome specific hybridization pattern of telomere probe (Cy5- $(CCCTAA)_3$) hybridized on CHO chromosomes compared to the background fluorescence in chromosomes hybridized without probe or with a non specific probe (Cy5- $(GCCTAA)_3$).

Supplementary figure 3
Parameters affecting Cy5 fluorescence signal for quantitative measurements of telomere repeats.

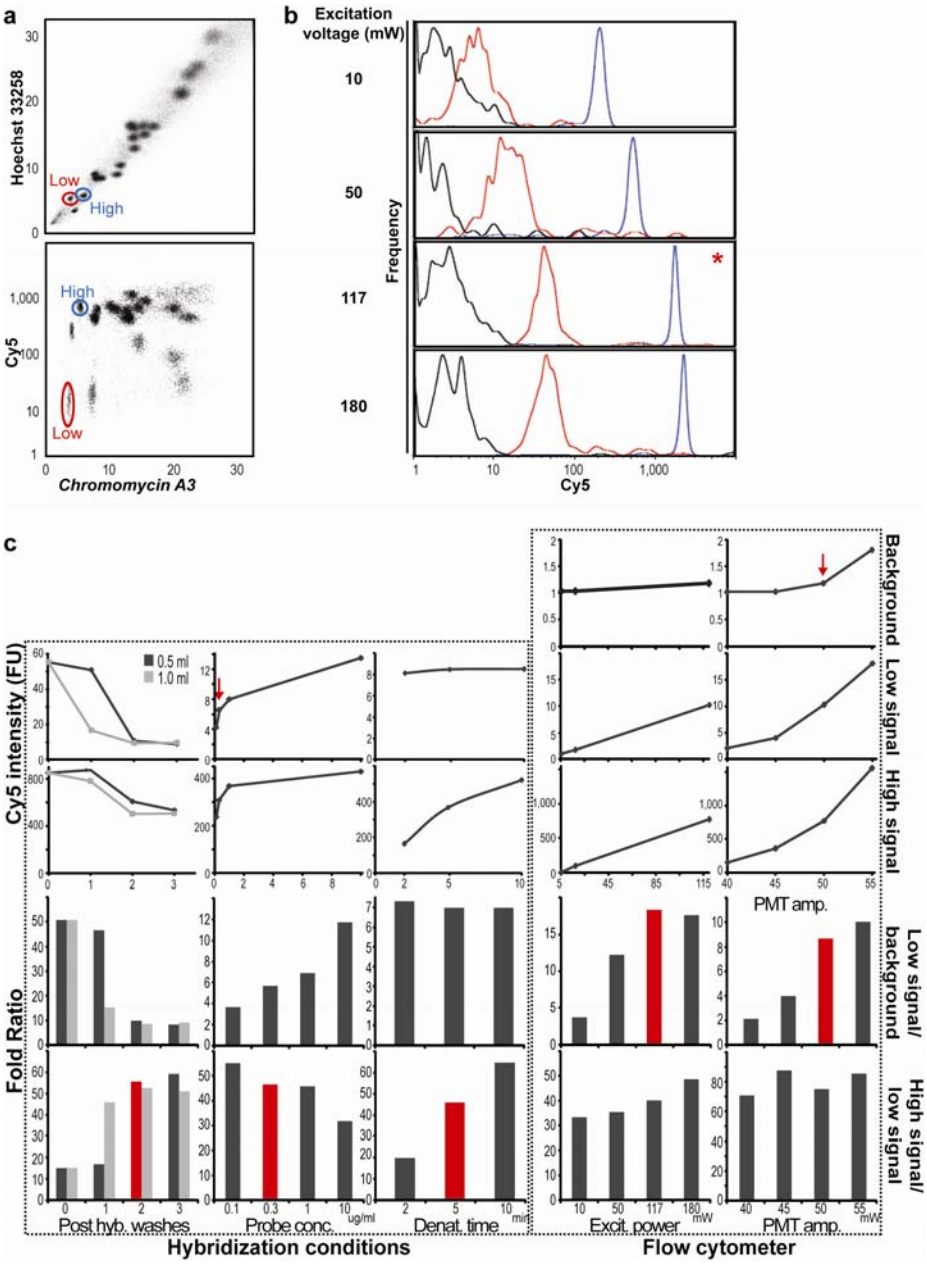

(**a**) Cy5/Chromomycin A3 flow karyograms of CHO chromosomes hybridized in suspension with a Cy5-labeled PNA telomere probe (Cy5- $(CCCTAA)_3$). Chromosomes with low (red) and high (blue) number of interstitial telomere sequences are shown. (**b**) Histograms representing background (black), low (red) and high (blue) Cy5 signal after varying 642 nM laser (Cy5) excitation power. The red star represents the selected optimal condition. (**c**) Selection of optimal hybridization conditions for quantitative measurements of telomere repeats using absolute signals discrimination of weak Cy5 signal above background and resolution of weak and strong signal of Cy5 fluorescence at different protocol parameters; number of post-hybridization washes, concentration of the probe, denaturation time, PMT power and excitation power. The red bar highlights the selected, optimal condition.

Supplementary figure 4
Improvements on Cy5 signal resolution and detection above background after optimization.

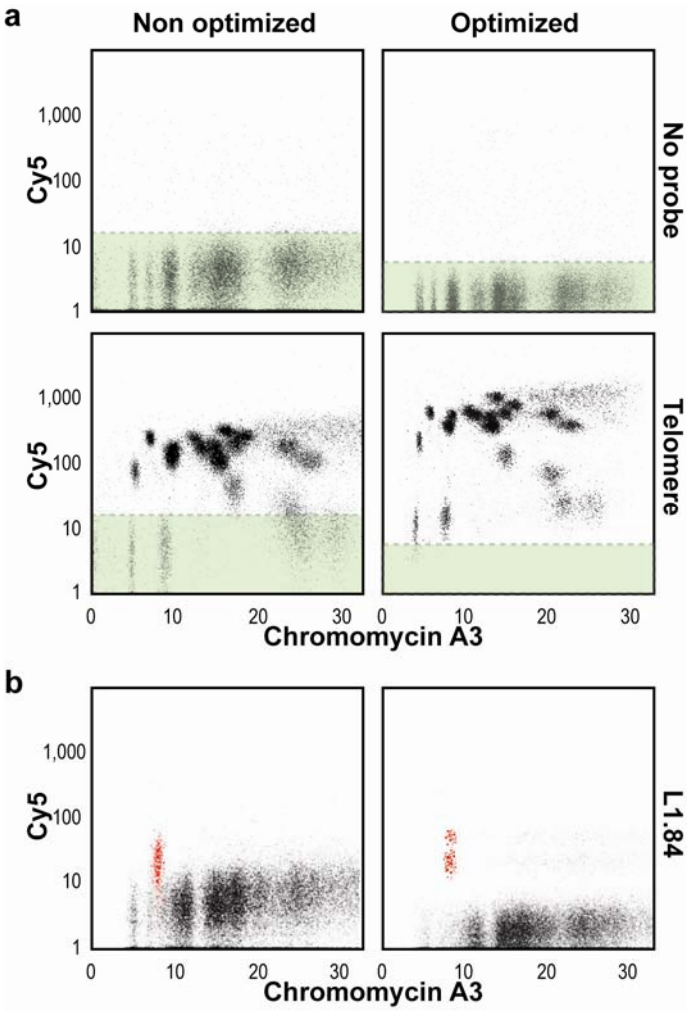

(**a**) Chromosome specific hybridization pattern in CHO compared to the background fluorescence in chromosomes hybridized with or without telomere probe before (Non optimized) and after (Optimized) selection of optimal hybridization conditions and instrument configuration. The green box represents the range of background signal. Non optimized conditions were 3 µg/ml probe, 5 minutes denaturation time and no post hybridization wash, 30mW 635 nm laser and 60 mW PMT amplification. Optimized conditions were 0.3 µg/ml probe, 5 minutes denaturation time and 2 post hybridization washes, 125mW 642 nm laser and 50 mW PMT amplification. (**b**) Detection of human chromosome 18 in HT1080 human chromosomes using a probe against the L1.84 alpha satellite sequence using optimized hybridization conditions with a 30 mW laser and 60 mW PMT amplification (left) or a 125 mW laser and 50 mW PMT amplification (right).

Supplementary figure 5

Comparison of chromosome flow FISH fluorescence measurements to Q-FISH quantitative measurements.

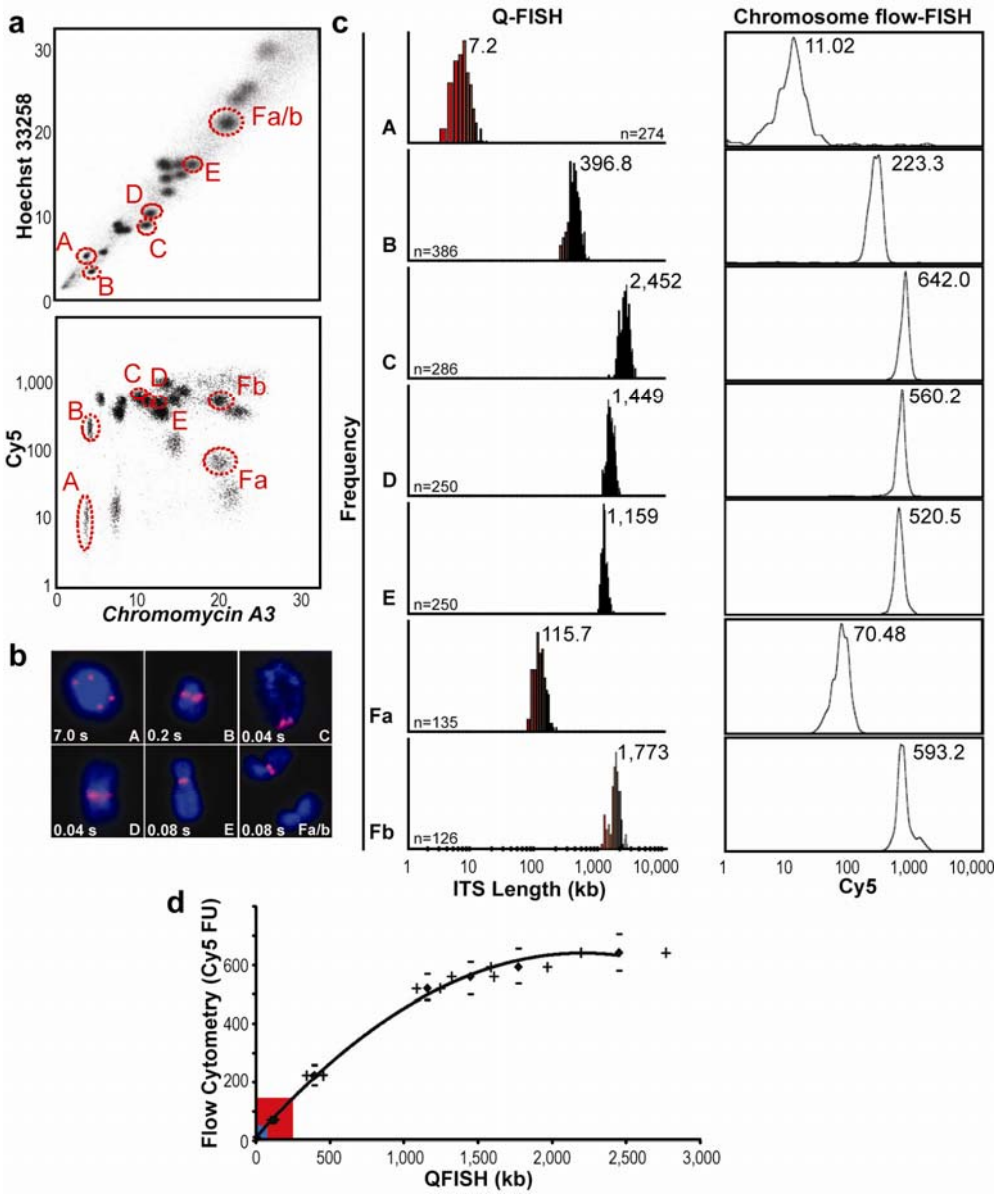

(**a**) Six CHO chromosome populations sorted on slides by FACS to quantify telomere repeats by Q-FISH. (**b**) Representative telomere Q-FISH images of the sorted chromosome populations. The sixth chromosome population (Fa and Fb) consists of two chromosomes not discriminated on the Hoechst/Chromomycin A3 bivariate flow karyotype, but that can be identified by their morphology on the microscope and by the different length of their interstitial telomeric sequences. (**c**) Telomere repeats measurements of the sorted chromosome populations by Q-FISH (telomere repeats length median in kb) and the Cy5 fluorescence emitted by those same populations measured by CFF (telomere fluorescence median in fluorescence units). (**d**) Correlation between the values obtained by Q-FISH and CFF for the same chromosome population. Mouse (red box) and human (blue box) range of whole chromosome telomere length are highlighted. FU: fluorescence units. u: Median , -: Cy5 FU 25/75th percentiles +: telomere repeat length (kb) 25/75th percentiles.

Supplementary figure 6
Distinct hybridization patterns of major satellite probe in mouse chromosomes.

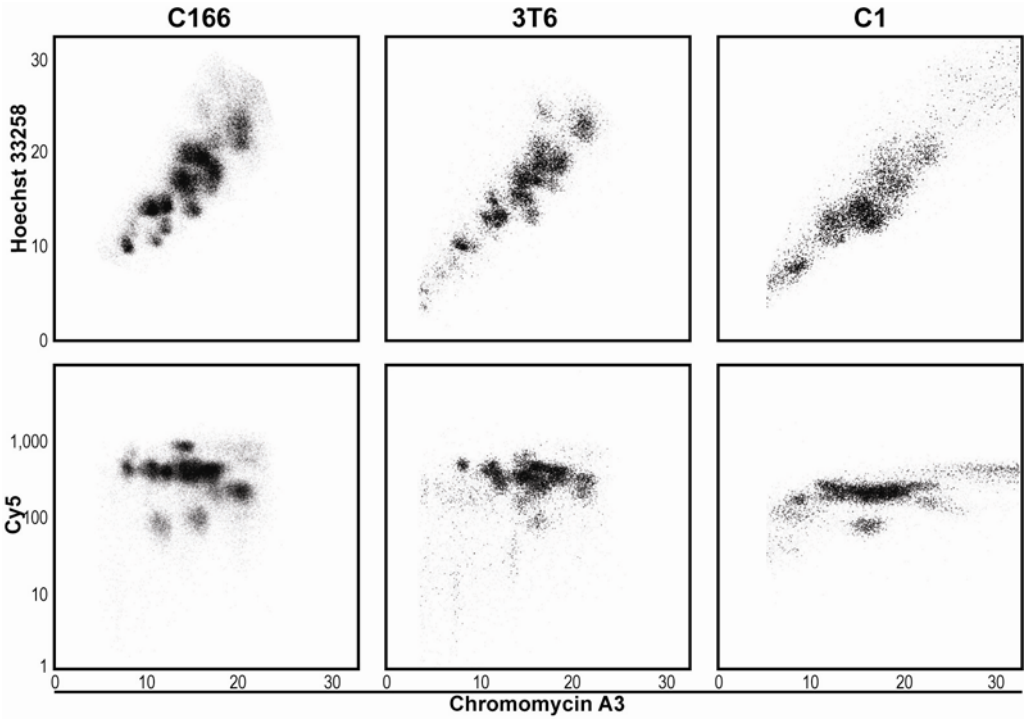

Hoechst 33258/Chromomycin A3 bivariate flow karyotypes and Cy5/Chromomycin A3 plots of chromosomes isolated from mouse cell lines from different backgrounds and hybridized with a major satellite PNA probe (Cy5-GACGTGGAATATGGCAAG). 3T6 (Swiss-albino fibroblasts), C166 (NMRI/GSF X CD-1 endothelial cells) and C1 (129/S embryonic stem cells).

Supplementary figure 7
Improved definition of poorly resolved chromosome populations in mouse flow karyograms.

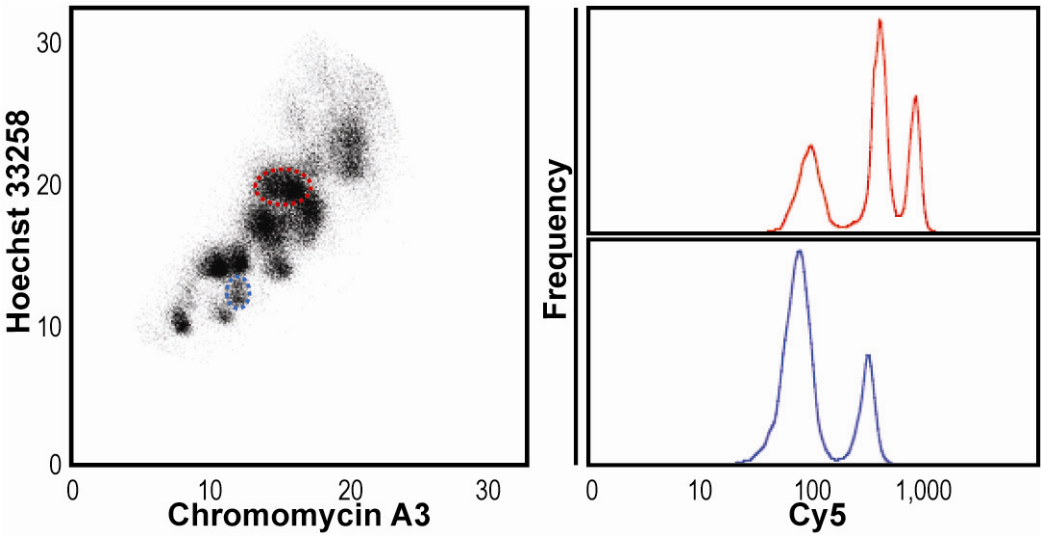

Hoechst/Chromomycin A3 bivariate flow karyogram of C166 (mouse) chromosomes hybridized with a major satellite PNA probe (Cy5-GACGTGGAATATGGCAAG). Cy5 fluorescence intensity histograms can resolve two poorly defined populations (red and blue) into three and two distinct populations respectively.

Supplementary figure 8
Gating strategy to remove debris from analysis plots.

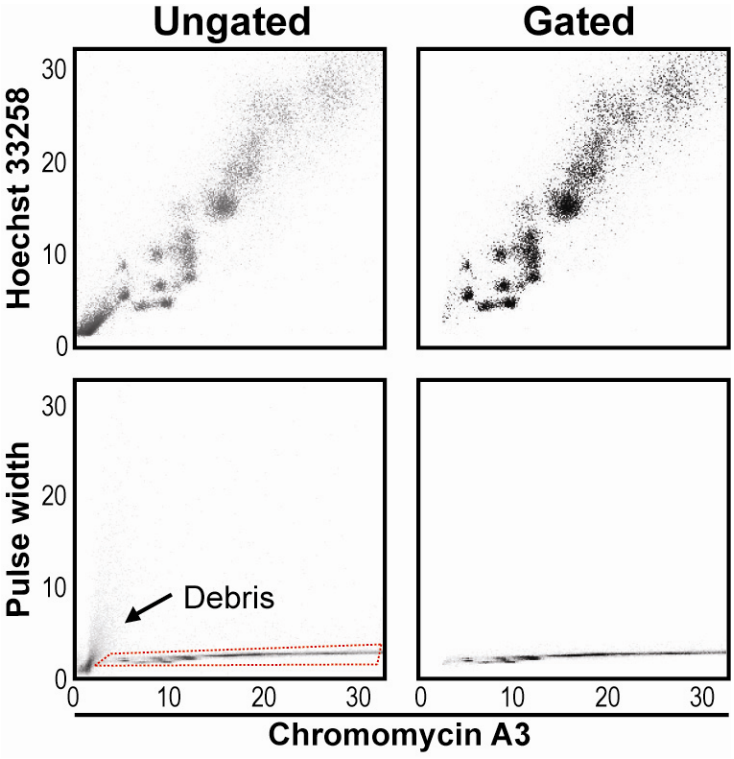

Gated and ungated Hoechst/Chromomycin A3 bivariate flow karyogram of HT1080 (human) chromosomes containing debris. Gating is performed on a Chromomycin A3/pulse width plot (debris present in the lower left corner).

SUPPLEMENTARY NOTE

Optimization of hybridization conditions

We optimized conditions to detect specific fluorescence from telomere repeats in CHO chromosomes as follows. First, we plotted absolute fluorescence emission intensities for a chromosome population with a low amount and a population with a high amount of fluorescence with the telomere probe (**Supplementary Fig. 3c**) to insure that a ratio increase was not due to a decrease in fluorescence specificity, especially where there is a low amount of signal. Additionally, we calculated the ratio of Cy5 fluorescence signal emitted by a population of chromosomes with a low amount of telomere signal (**Supplementary Fig. 3a**, red) over the background fluorescence (no probe control) to select conditions favoring reproducible detection of weak fluorescence. Similarly, we optimized the signal resolution by selecting conditions that maximize the ratio of fluorescence emitted by chromosomes with a bright telomere fluorescence (**Supplementary Fig. 3a**, blue) over the fluorescence emitted by chromosomes with low fluorescence (red). Using this approach, we evaluated various parameters involved in the hybridization process, including the number and volume of post hybridization washes, probe concentration and denaturation time (**Supplementary figure 3b** and **c**). We selected hybridization conditions with an emphasis on fluorescence specificity and resolution of signal. For example, when optimizing probe concentration, using more probe increases the low signal/background ratio (bottom histogram), but the increase in low fluorescence signal is not proportional to the increase in probe concentration (top curve), indicating that the increase in low fluorescence signal is due to non specific binding of the probe. We determined the best conditions to be 5 minutes heat denaturation at 80°C in the presence of 0.3 µg/ml telomere Cy5 PNA probe, followed by hybridization for 60 minutes at 37°C and two 0.5 ml post hybridization washes at 37°C.

Optimization of flow cytometry settings

We used similar criteria to determine the optimal instrument configuration and setting for the flow cytometer. To investigate if CFF measurements were limited by the number of excitation photons, we measured telomere fluorescence at different laser power using different lasers and neutral density filters. The ability to distinguish weak fluorescence from background fluorescence improved with increased laser power for excitation of the Cy5 dye in the telomere probe (**Supplementary Fig. 3b and c**), in agreement with a previous study that demonstrated an improved resolution of chromosome populations in Hoechst 33258/Chromomycin A3 bivariate flow karyograms with increasing laser power[20]. We obtained an optimal excitation at 117mW of 642nm light, significantly more than generated by the most common lasers used to excite Cy5 in flow cytometers. Changes in the photomultiplier tubes (PMT) settings had no effect on the resolution of bright versus weak signals (**Supplementary Fig. 3c**), indicating that fluorescence detection is not limited by PMTs in our instrument in the power range tested. It is important to note that increasing PMT power is an amplification procedure that will also increase the background fluorescence (**Supplementary Fig. 3c**, top curve).We determined an excitation power of 117 mW and a PMT power of 50 mW to be optimal to detect weak Cy5 fluorescence signal above background while preserving the resolution of bright signal. When using a lower laser excitation power, PMT power can be further increased to detect populations with weaker fluorescence intensities from background, but it can be at the cost of resolution between populations of similar fluorescence intensities (**Supplementary Fig. 4b**).

Correlation of between measurements by chromosome flow FISH and Q-FISH

We validated the potential of CFF for quantitative measurements of telomere repeats by comparing CFF to Q-FISH, the current standard for chromosome specific telomere length measurements. We sorted six specific chromosome populations by fluorescence activated cell sorting (FACS) (**Supplementary Fig. 5a**)

and fixed them onto slides. Representative Q-FISH images for each of the six sorted chromosome populations are presented in **Supplementary Figure 5b** and individual telomere measurement histograms for each of these sorted populations are available in **Supplementary Figure 5c**. Note that the sixth sorted population (population F) corresponds to two distinct chromosomes (Fa and Fb) which cannot be discriminated on the bivariate Hoechst 33258 and Chromomycin A3 flow karyotype, but which are easily identifiable by microscopy (**Supplementary Fig. 5b**) and CFF (**Supplementary Fig. 5a**). CFF measurements correlated with Q-FISH measurements (Pearson's = 0.9847) (**Supplementary Fig. 5d**), highlighting the potential of CFF for quantitative analysis of repeat numbers on specific chromosomes. However, note that the weak fluorescence signal is near the limit of resolution of our current CFF method (**Supplementary Fig. 5d**).

SUPPLEMENTARY REFERENCE

20. Ng BL, Carter NP. *Cytometry A* **77**, 585-588 (2010).